

PAPER

Shape memory polymer/CNT composites and their microwave induced shape memory behaviors

Cite this: *RSC Adv.*, 2014, 4, 2961Kai Yu,^a Yanju Liu^b and Jinsong Leng^{*a}

In this paper, the practicability of actuating the shape recovery of thermo-responsive shape memory polymers (SMPs) filled with carbon nanotubes (CNTs) has been investigated. When exposed to microwave radiation, the embedded CNTs were expected to absorb the external electromagnetic energy and act as node heating sources in the SMP/CNT composites. In this way, the SMP could be volumetrically heated and subsequently this would lead to a fast actuation. Although the pure SMP was not responsive to microwave radiation, the microwave absorption ratio in the SMP/CNT composites significantly increased along with the increasing amount of added CNTs or the microwave frequency. The influence of the CNTs on the thermomechanical properties of the SMP composites has been investigated and analyzed using scanning calorimetry (DSC) and dynamic mechanical analysis (DMA) methods. The shape recovery behaviors of the SMP composites with 1 wt%, 3 wt% and 5 wt% CNTs were successfully triggered by microwave radiation. The shape recovery process together with the temperature distribution were recorded with an infrared video camera simultaneously. Furthermore, the selective heating characteristic of the microwaves was also experimentally demonstrated on a SMP composite with a nonuniform CNT concentration. The microwave actuation method is potentially a better choice for the wireless remote shape control of SMP/CNT based functional structures.

Received 27th June 2013
Accepted 14th October 2013

DOI: 10.1039/c3ra43258k

www.rsc.org/advances

1. Introduction

As an emerging class of smart polymer, shape memory polymers (SMPs) have gained extensive research interest lately due to their excellent properties, such as the high recoverable strain (up to 1000%),¹ low density, low cost, easy shape procedure and easy control of recovery temperature.² The shape memory effect of SMPs refers to their capability to recover their original shapes in the presence of external stimuli,³ such as electricity,^{4–10} light,¹¹ magnetic fields^{12–15} and solvents.^{16–19} SMPs have been designed into actuators or sensors providing remarkable advantages and are widely used in medical, civil and industrial applications.

Various actuation methods of SMPs have been developed based on the diverse stimuli that SMPs are responsive to. However, a specified actuation method of SMPs may be infeasible in some practical applications. For example, it is usually impossible to immerse structural components of SMPs into solvents during operation. Joule heating, generated by electric and magnetic energy, is generally regarded as a convenient method for the actuation of SMPs. However the fact that direct contact between the material and the electrode is necessary

strongly restricts their further application in certain environments (biomedical, aerospace, *etc.*), where non-contact and distant actuation of SMPs is required.¹⁴ For the light actuation of SMPs, the penetration depth is unsatisfied. Only the material surface is heated. Heat then has to transfer to the inside of the SMPs by thermal conduction. The heating efficiency is low if the SMP components have large dimensions. In these cases, microwave actuation is considered to be a better choice. In comparison with other electromagnetic waves, microwaves have a long wavelength and hence possess better penetrability. On the other hand, due to the low attenuation degree during transportation, microwaves can actuate SMPs from a relatively long distance without considerable energy loss. These properties of microwaves offer the opportunity to induce thermal-responsive SMPs wirelessly and from a distance.

Since microwaves show no heating effects on pure SMPs, it is necessary to introduce microwave energy absorbers into SMPs. Previously, microwave induced polymer shape memory effects were achieved in studies by Du *et al.*²⁰ and Xu *et al.*²¹ where water molecules and T-ZnOw nanoparticles were respectively designed as microwave energy absorbers. Some ferroelectric nanoparticles (such as BaTiO₃) have also been considered as reinforcements for polymer composites,^{22–27} which subsequently improved their microwave properties and potential shape memory effects. In our study, carbon nanotubes (CNTs) were selected as the additives not only because of their superb electrical, mechanical and thermal properties,²⁸ but also

^aCentre for Composite Materials, Science Park of Harbin Institute of Technology (HIT), P.O. Box 3011, No. 2 Yikuang Street, Harbin, P. R. China. E-mail: lengjs@hit.edu.cn

^bDepartment of Astronautical Science and Mechanics, Harbin Institute of Technology (HIT), P.O. Box 301, No. 92 West dazhi Street, Harbin, P. R. China

because of their strong microwave absorbing ability.²⁹ Even though the interaction mechanism between CNTs and microwaves is not completely understood and various possibilities (CNT impurities,^{30–33} generation of gas plasma,³⁴ and dipolar polarization^{35,36}) have been reported, the strong absorption phenomenon of CNTs has been observed in different composites and blends. Generally, the excessive heating effect is regarded as evidence for microwave absorption of CNTs. Under vacuum, T. J. Imholt *et al.*³⁴ observed that in a 700 W, 2.45 Hz microwave field, CNTs were heated to a temperature of 1550 °C. By measuring the heating rate of the CNT dispersion in silicone oil, K. R. Paton *et al.*³² experimentally proved that adding as little as 0.04 wt% CNTs into the silicone oil enhanced the microwave absorbance of the silicone oil by 500 times. A. L. Higginbotham *et al.*³⁷ also observed that bulk ceramic/CNT composites demonstrated rapid initial heating rates. Typically, the composite with less than 1 wt% CNT additive was heated to 500 °C within 1 min with 30–40 W directed microwave (2.45 GHz) irradiation.

The current work aims to find a practical remote controllable actuation method to use for SMP devices. The CNTs added into the polymer matrix played important roles as the microwave absorbers and transformed the electromagnetic energy into heat. Therefore, the SMP matrix could subsequently be heated using numerous internal thermal sources with a high heating efficiency. The microwave absorption efficiency of the SMP/CNT composites with different amounts of CNTs, the influence of the CNTs on the thermomechanical properties of the SMP/CNT composites, as well as the actuation and selective heating effect of microwave radiation on the investigated SMP/CNT composites have been investigated and analyzed experimentally.

2. SMP/CNT composites

2.1. Materials

In the current study, a styrene-based shape memory resin (Veriflex®S VF 62) with a density of 0.92 g cm⁻³, as well as its curing agent (dibenzoyl peroxide hardener) were both purchased from Cornerstone Research Group, Inc. (USA). This is a two-part, fully formable thermoset SMP resin system, engineered with a glass transition temperature (T_g) of 62 °C. The detailed mechanical and thermal properties of this styrene SMP are listed in Table 1. The multi-walled CNTs were purchased from Shenzhen Nanometer Gang Co., Ltd. (China), with an estimated average length of 1 µm and an estimated average diameter of 50 nm.

2.2. Fabrication of SMP/CNT composites

The SMP/CNT composites with different CNT concentrations (1 wt%, 3 wt % and 5 wt %) were prepared for our current study.† The fabrication procedure was as follows. First, the shape memory resin was mixed with the crosslinking agent at a weight ratio of 24 : 1. Second, the CNTs were mixed with the

Table 1 Mechanical and thermal properties of the thermosetting styrene based SMP

Mechanical properties	Value	Method
Tensile strength	22.96 MPa	ASTM D638
Tensile modulus	1241.1 MPa	ASTM D638
Tensile elongation to break	3.90%	ASTM D638
Flexural strength	31.72 MPa	ASTM D790
Flexural modulus	1241.1 MPa	ASTM D790
Thermal properties		Value
Glass transition temperature	143 °F/62 °C	
Thermal conductivity @ 18.9 °C	0.17 W m ⁻¹ K ⁻¹	

resin mixture with stirring. Then the resin/CNT suspension was placed in a high-energy sonicator (SONICS-44349N) with an output amplitude of 60% for a total of 40 min, in intervals of 10 min. Third, the mixture was placed in an air-tightened box to completely remove the air bubble, and then transferred into a close mould. Finally, the resin mixture was cured in an oven in three heating steps: the temperature was increased with a ramp of approximately 1 °C min⁻¹ from room temperature to 75 °C, then the temperature was held at 75 °C for 3 hours before being ramped to 90 °C at a rate of 15 °C 180 min⁻¹, the temperature was then ramped to 110 °C at a rate of 20 °C 120 min⁻¹.

3. Results and discussion

3.1. Structure of the SMP composites

The microcosmic morphologies of the SMP/CNT composites were observed through a scanning electron microscope (SEM), Camscan, MX2600. The details of the morphology of the SMP/CNT composite incorporated with 1 wt% CNTs are shown in Fig. 1. It can be observed that the CNTs exhibited a relatively good dispersion in the SMP, and were distributed randomly and separately. Since the embedded CNTs were expected to act as internal thermal sources under microwave energy, a good dispersion should lead to a homogeneous heating effect in the SMP materials.



Fig. 1 Morphology of the SMP composite with 1 wt% of CNTs.

† In our study, SMP composites with CNT contents higher than 5 wt% were not used because our previous investigations indicated that excessive amounts of CNTs would increasingly inhibit the polymerization reaction of the styrene based shape memory resin.

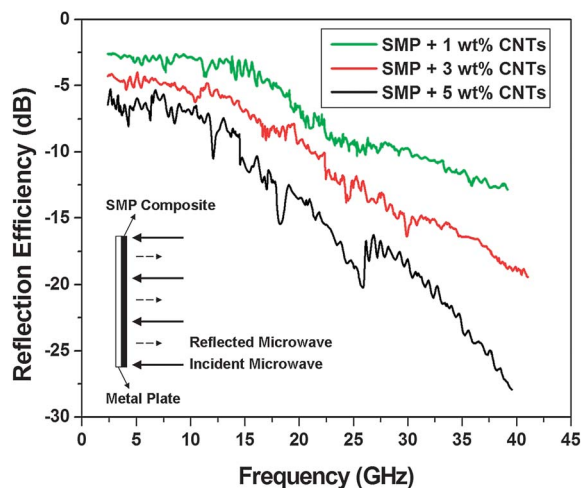


Fig. 2 Microwave reflection efficiency (E_R) versus microwave frequency.

3.2. Microwave absorption properties of the SMP/CNT composites

The microwave absorption properties of the SMP/CNT composites with different amounts of CNTs was measured by the Radar Absorbing Material Reflectivity Far-Field Radar Cross Section Method. A vector network analyzer (Agilent 8722ES) was used for the data recording and analysis. The tests were carried out under a microwave frequency ranging from 2.4 GHz to 40 GHz. The bottom-left inset in Fig. 2 illustrates a schematic representation for measuring the microwave absorption ability of the composites. At the surface of the tested specimen, each incident microwave is divided into the reflected microwave and the absorbed microwave.^{†38} In the following equation, we denote P_I as the power density of the incident microwave, P_R as the power density of the reflected microwave, and P_A as the power density of the absorbed microwave.

$$P_I = P_R + P_A \quad (1)$$

During the test, P_I was a constant value and P_R was recorded by the vector network analyzer. For convenience, the microwave reflection efficiency (E_R) is introduced and was calculated in decibels (dB) using the following equation.

$$E_R = 10 \log(P_R/P_I) \quad (2)$$

Then, the microwave absorption ratio is given by the following equation:

$$E_A = (P_I - P_R)/P_I \times 100\% \quad (3)$$

[†] During the experiment, the SMP specimen was placed in the testing equipment, with the direction of the incident microwave consistent with the normal direction of the specimen with a flat surface, and hence the microwave scattering was minimized and negligible.

Based on eqn (1), (2) and (3), it was concluded that the microwave absorption properties of the SMP/CNT composites could be characterized by E_R and E_A . The microwave absorption ability increased along with increases in the absolute values of E_R and E_A .

The relationship between the microwave reflection efficiency and the microwave frequency is revealed in Fig. 2. Under a specified frequency, the absolute value of E_R was observed to increase along with the addition of CNT content. Compared with the SMP composite with 1 wt% CNTs, an average increase of 100% in the absolute value of E_R was observed in the SMP composite with 5 wt% CNTs. On the other hand, for each SMP/CNT specimen, the absolute value of E_R increased remarkably with an increase in the microwave frequency. Fig. 3 presents the microwave absorption ratios of different specimens over the same microwave frequency range. The data was calculated based on eqn (3). While the absorption ratio fluctuated in the low frequency range (2.4–17 GHz), a steady increase was observed in the high frequency range. At a frequency of 2.4 GHz, the microwave absorption ratios of the SMP composites with 1 wt%, 3 wt% and 5 wt% CNTs were 44.82%, 62.81% and 77.32% respectively, and they increased to 94.82%, 98.85% and 99.84% respectively at a frequency of 40 GHz.

The test results illustrate that the CNTs exhibit a good microwave absorption ability at high microwave frequencies, where most of the microwave energy is absorbed instead of reflected at the surface of the SMP composites. For the SMP composites with low CNT concentrations, the moderate microwave absorption abilities result from the limited amount of microwave absorbers in the composites, rather than the microwave absorption ability of a single CNT playing the dominant role. CNTs are proven to be excellent microwave absorbers in the investigated SMP composites.

3.3. Glass transition characteristics of the SMP/CNT composites

The glass transition temperature (T_g) of a non-crystalline material refers to the critical temperature at which the material

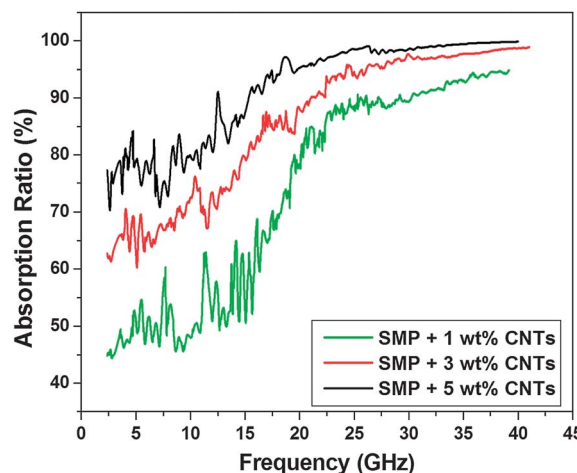


Fig. 3 Microwave absorption ratio versus microwave frequency.

changes its behavior from being glassy to being rubbery. When it comes to SMPs, T_g is the switching temperature where the modulus of SMP begins to significantly decrease and the SMP begins to show the shape memory effect. Therefore, T_g plays an essential role in the shape memory process for SMPs and SMP based composites. Thus, it was necessary to measure T_g prior to the shape memory behavior investigations of the SMP/CNT composites.

Differential scanning calorimetry (DSC) measurements are routinely employed to detect the transition temperature of polymers. In our current study, a Netzsch Instrument DSC 204F1 was used to investigate the thermal properties of the composites in a nitrogen environment. Since the glass transition always occurred over a temperature range, the midpoint of the temperature range in the scanning curve was defined as T_g in this study. The specimens were heated from -20 to 150 °C, then cooled down to -20 °C, and again heated up to 150 °C at a scanning rate of 10 °C min^{-1} . The thermal transitions in the second thermal scan were used for analysis.

The T_g values of all the SMP/CNT specimens are presented in Fig. 4 as a function of the CNT content. For a clearer illustration, the T_g values (together with the onset and end point of the glass transition) are also summarized in Table 2. Compared with the T_g value of the pure SMP (62 °C), the T_g value of the SMP/CNT composites decreased from 60.7 °C to 52.9 °C with the addition of CNTs from 1 wt% to 5 wt%. With the increase in the content of CNTs, the glass transition shifted a little towards a lower temperature range. This is because the relative motion of the macromolecule segments is the primary mechanism of the glass transition and shape memory effect in SMPs. When we gradually increased the amount of CNTs, which have superb conductivity properties, the amount of SMP segments per unit volume in the composite as well as the thermal conduction pathway between neighboring CNTs were both reduced. Therefore, the thermal response of the SMP composite was faster, and the thermal conductivity was higher. During the experiments, with the same amount of energy, the mobility of

Table 2 Critical temperature points (onset point, half-height (T_g) and end point) during the glass transition processes of the SMP composites by DSC characterization

	SMP + 1 wt% CNT	SMP + 3 wt% CNT	SMP + 5 wt% CNT
Onset point (°C)	49.2	47.6	43.2
Half-height, T_g (°C)	60.7	57.8	52.9
End point (°C)	73.7	69.1	62.4

the polymer chains in the SMP composite was expected to be higher than in the pure SMP, which would subsequently lead to a lower glass transition temperature. Experimental measurements also revealed that the glass transition occurred within a narrow temperature range when the CNT content was increased to 5 wt%. It can be concluded that after embedding CNTs into the SMP, the thermal actuation of the SMP composite tended to be faster and easier.

3.4. Dynamic mechanical performance of the SMP/CNT composites

The storage modulus of a SMP/CNT composite measures the stored energy in the viscoelastic state, representing the elastic portion of the material. This data could be used to calculate the shape recovery stress under various loading conditions. Here, the dynamic mechanical properties were tested on a Netzsch DMA 242C (Netzsch, Germany) and the storage moduli of the composites as a function of temperature were obtained. All specimens were tested in a three-point bending mode with a constant heating rate of 10 °C min^{-1} . The scanning temperature ranged from 20 to 120 °C and the oscillation frequency was 1 Hz. Specimens with dimensions of $80 \times 15 \times 1.5$ mm³ were initially locked into a deformation of 0% with zero initial force.

As previously revealed by Fu *et al.*,³⁹ nano-sized reinforcements typically exhibit effective enhancements to the strength and Young's moduli of composite SMPs, at the expense of slightly reduced recovery rates. Besides, the material stretch ability and thermal properties will be affected at the same time. In this section, we limit ourselves to revealing the modulus improvement in the SMP/CNT composites. As shown in Fig. 5, where the storage modulus is recorded against the temperature, at a temperature of 20 °C, the storage modulus of the SMP/CNT composites increased remarkably with the addition of CNTs. This can be attributed to the ultrahigh elastic modulus of CNTs (over 1 TPa),^{40–43} as well as the superior bonding between the CNTs and SMP matrix.^{44–47} Therefore, the mechanical properties of the SMP composite were improved significantly with only a slight amount of CNTs. In the meantime, it was found that the storage modulus of each SMP/CNT specimen below the T_g value was about two orders of magnitude larger than that above the T_g value. For instance, the SMP composite with 5 wt% CNTs exhibited a storage modulus of 2295.7 MPa at 20 °C, while it is just 112.787 MPa at 100 °C. On the other hand, for the pure SMP and the SMP composites with 1 wt% and 3 wt% CNTs, the storage modulus increased along with the addition of CNTs over the entire temperature range. This is because the size of typical

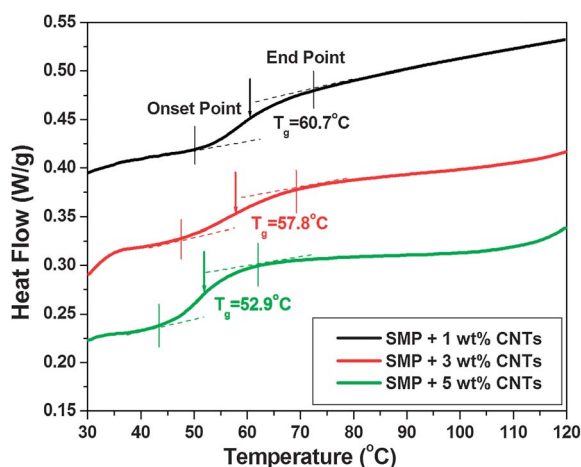


Fig. 4 Thermal curve of the SMP composites after quenching with the glass transition temperatures calculated using the half-height.

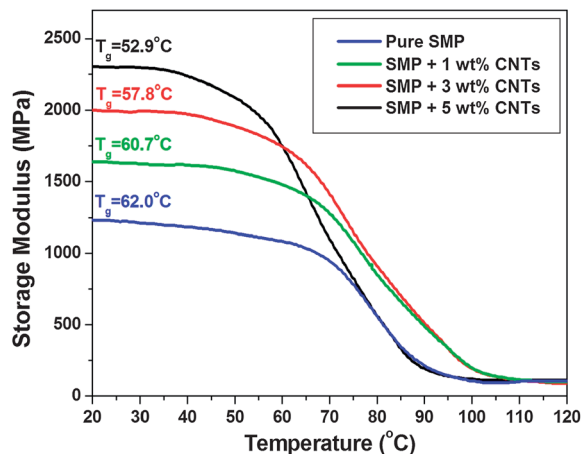


Fig. 5 Storage modulus as a function of temperature for the SMP composites.

segments in the polymer network were approximately 10–100 nm, which is of the same order of magnitude as the typical size of CNTs. Thus, the mechanical and thermo-mechanical behavior of the segments were prevented by these nano-sized fillers. These interactions are considered as friction interactions that would help the SMP/CNT composites to resist external loading, resulting in improved mechanical and thermomechanical properties. A higher shape recovery stress was generated in SMP composites with higher CNT concentrations. Our previous research demonstrated that excessive CNT content would inhibit the polymerization reaction of the styrene based shape memory resin, and this may explain why the storage modulus of the SMP composite embedded with 5 wt% CNTs decreased faster than the others.

3.5. Thermal conductivity of the SMP/CNT composites

Thermal conductivity indicates the ability of a material to conduct heat. Traditionally, polymeric materials possess an intrinsically low thermal conductivity of the order of $0.15 < k < 0.30 \text{ W mK}^{-1}$ for most cases, which makes them good insulators for numerous applications. However, for thermal responsive SMP composites using internal heating, a relatively high conductivity is required. It has previously been revealed by the authors that the total shape recovery time of such SMP composites is the summation of the initial thermal conduction (spread from each heating source to its neighbors) time and the intrinsic shape recovery time of the subsequent material. For the studied SMP/CNT composites, when the amount of CNTs was gradually increased, the time spent on the initial thermal conduction decreased due to the minimized thermal conduction pathway within the system, which rendered a fast thermal response and shape changing in the SMP composite. Fig. 6 presents the relationship between thermal conductivity and the weight fraction of CNTs. The thermal conductivity of the pure SMP was approximately 0.17 W mK^{-1} at room temperature. In comparison, the SMP composites possessed higher thermal conductivities and the values proportionally increased with the

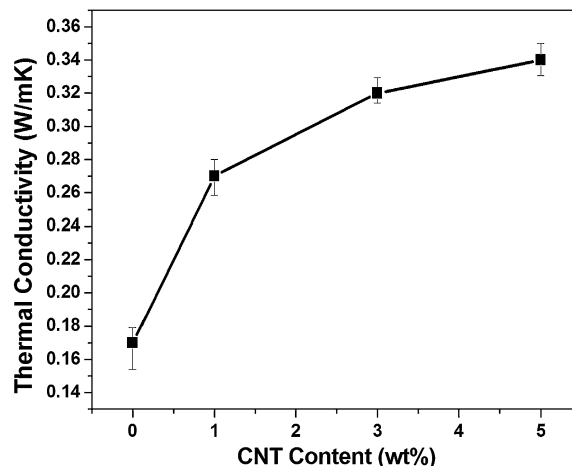


Fig. 6 Thermal conductivity as a function of CNTs weight fraction for the composites.

addition of CNTs. The thermal conductivity of the SMP composites increased to 0.33 W mK^{-1} with 5 wt% CNTs. This increase suggests that the CNTs are beneficial as components in SMPs with respect to the thermal conductivity and thermal responses.

3.6. Microwave actuation of the SMP/CNT composites

To demonstrate the feasibility of microwave actuation of the SMP composites, specimens with dimension of $70 \times 20 \times 5 \text{ mm}^3$ were cut out from the fabricated SMP composites and exposed to a microwave field. A domestic microwave oven (MG-5013 TW) with proper modifications was selected as the radiation source because of its easy availability. The output microwave power was adjusted to 120 W, with a frequency of 2.45 GHz. The distance between the permatron and the specimen was 25 cm. Before carrying out the shape recovery test, each SMP/CNT specimen was bent into a V shape at a temperature of 100°C , and then cooled to 25°C . One side of the V shaped specimen was fixed under the permatron in the microwave oven. An infrared video camera (AGEMA, Thermo-vision 900) was used in our study to monitor the temperature distribution and shape recovery behavior simultaneously.

Following the same shape memory cycle that was previously designed by the authors,² all the specimens were firstly bent around a mandrel at the specified programming temperature ($T_g + 20^\circ\text{C}$), and then the external load was removed after the specimens were cooled down to room temperature. As discussed by Huang *et al.*,⁴⁸ when SMPs are programmed at a temperature that is high above the glass transition temperature, the associated shape fixity after unloading is expected to be close to 100%. The microwave induced free recovery process, as well as the time dependent shape recovery ratio (R_t), is shown in Fig. 7. The microwave induced heating began to yield quickly after the microwave radiated for 2 s. The SMP/CNT specimens with higher CNT weight fractions exhibited higher heating efficiencies under microwave radiation. This is because more microwave energy is absorbed and transformed into thermal

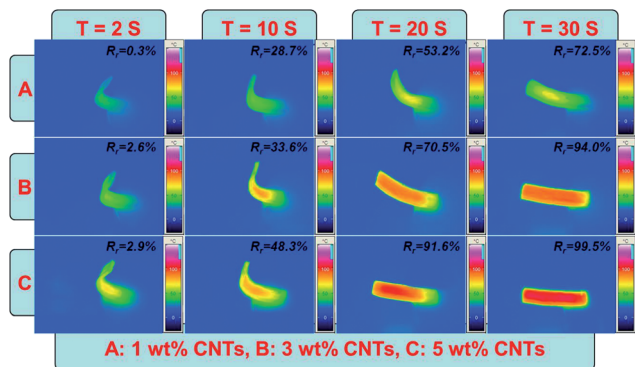


Fig. 7 Sequence of the shape recovery process of the SMP composites under microwave radiation (2.45 GHz).

energy within the same radiation time. After 30 s, the SMP composite specimens with 3 wt% and 5 wt% CNTs fully recovered their original shapes, and maximum temperatures of 90.5 °C and 109.8 °C were reached respectively, which far exceeded their corresponding transition temperatures. However the recovered shape in the SMP composite specimen with 1 wt% CNTs was lower than 80%, and the highest temperature was lower than 62 °C. The remaining deformation in the shape might have resulted from an insufficient amount of microwave energy absorbed in the SMP composite for overcoming the friction among the CNTs and the soft segments in the polymer network. Furthermore, it must also be noted that the rate of shape recovery was strongly dependent on the magnitude of the applied microwave power in the microwave oven.

On the other hand, because the microwave heated the material volumetrically, the heating effect could be homogeneous if the internal reinforcement was uniformly distributed.^{49–52} As shown in Fig. 7, a homogeneous heating phenomenon was observed in the SMP specimens with 3 wt% and 5 wt% CNTs during the experiments. Moreover, there were no significant temperature gradients within the materials and

so no residual stress was generated during the microwave actuation of the SMP composites.

To demonstrate the selective heating effect of the microwave field, a nonuniform SMP/CNT composite was fabricated. The specimen with a total thickness of 2 mm was composed of 1 mm of pure SMP and 1 mm of the composite with 3 wt% CNTs. A specimen with dimensions of $90 \times 20 \times 2 \text{ mm}^3$ was then cut and prestretched by about 10% in length at a temperature of 100 °C. After cooling to room temperature, one end of the stretched specimen was fixed in the microwave oven for testing. The radiation microwave power used was 40 W with a frequency of 2.45 GHz. The infrared video camera was also applied during the test to monitor the temperature distribution and the shape recovery process.

Fig. 8(a) is a schematic diagram for the experiment. Under a microwave field, the CNTs in the SMP composite absorb the external electromagnetic energy and heat the surrounding SMP matrix. When the SMP matrix is heated above the glass transition temperature, it begins to recover its shape and constrict in length. At the same time, the pure SMP part could not be heated. Therefore, an inhomogeneous strain was generated in the SMP/CNT composite, and the specimen wrapped up. As shown in Fig. 8(b), the specimen began to deform at about 5 s after microwave irradiation. After 30 s, no more bending deformation was observed, and the bending angle was approximately 50°. Further exposure to the microwave field led to a decrease in the bending angle, which was a result of thermal conduction from the composite part to the pure SMP part. The selective heating effect of the microwave can be utilized to actuate nonuniform SMPs into specified shapes.

4. Conclusions

This paper presents a novel actuation method for SMP composites filled with CNTs. After exposure to a microwave field, the embedded CNTs absorbed the external electromagnetic energy and transmitted it into heat to thermally induce shape recovery in the SMP/CNT composites. The absorption ratio increased along with the addition of CNTs and the microwave frequency. At a frequency of 40 GHz, 99.84% of the microwave energy could be absorbed into the SMP composite with 5 wt% CNTs. DSC investigations on the SMP/CNT composites revealed that the T_g values decreased from 62 °C to 52.9 °C when increasing the CNT content from 0 to 5 wt%. The decreased T_g values and the relatively narrower glass transition temperature ranges offered benefits for the microwave actuation of SMP/CNT composites. Results from the DMA tests and the thermal conductivity measurements also proved that the embedded CNTs positively enhanced the thermomechanical and thermal properties of the SMP composites. Finally, under microwave radiation (40 W, 2.45 GHz), the shape recovery of SMP/CNT composite specimens were successfully induced. Due to the intrinsic properties of microwaves (higher wavelength, low attenuation degree, *etc.*), this is considered to be an ideal method for the rapid remote and wireless actuation of SMP/CNT composites.

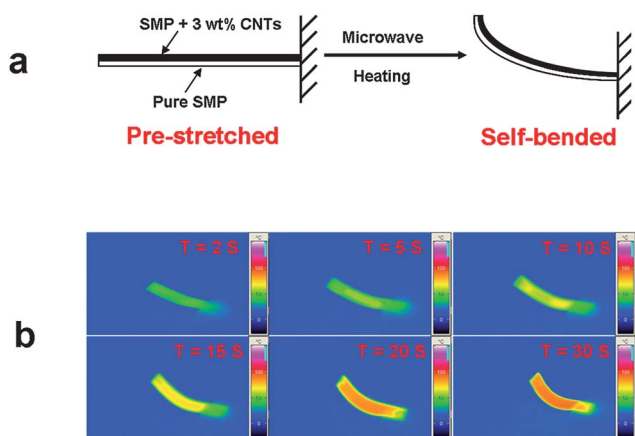


Fig. 8 Sequence of the shape recovery of a SMP composite with a nonuniform CNT concentration: (a) an experimental schematic, (b) infrared record of the shape recovery process.

References

- 1 M. Ahmad, *et al.*, Synthesis and Characterization of Polyurethane-Based Shape-Memory Polymers for Tailored T_g around Body Temperature for Medical Applications, *Macromol. Chem. Phys.*, 2011, **212**(6), 592–602.
- 2 X. Lan, *et al.*, Fiber reinforced shape-memory polymer composite and its application in a deployable hinge, *Smart Mater. Struct.*, 2009, **18**(2), 024002.
- 3 J. S. Leng, *et al.*, Shape-memory polymers and their composites: Stimulus methods and applications, *Prog. Mater. Sci.*, 2011, **56**(7), 1077–1135.
- 4 J. S. Leng, *et al.*, Electrical conductivity of thermoresponsive shape-memory polymer with embedded micron sized Ni powder chains, *Appl. Phys. Lett.*, 2008, **92**(1), 014104.
- 5 J. S. Leng, *et al.*, Significantly reducing electrical resistivity by forming conductive Ni chains in a polyurethane shape-memory polymer/carbon-black composite, *Appl. Phys. Lett.*, 2008, **92**(20), 204101.
- 6 J. S. Leng, *et al.*, Synergic effect of carbon black and short carbon fiber on shape memory polymer actuation by electricity, *J. Appl. Phys.*, 2008, **104**(10), 104917.
- 7 H. B. Lu, *et al.*, Electroactive shape-memory polymer nanocomposites incorporating carbon nanofiber paper, *Int. J. Smart Nano Mater.*, 2010, **1**(1), 2–12.
- 8 J. S. Leng, *et al.*, Electroactive thermoset shape memory polymer nanocomposite filled with nanocarbon powders, *Smart Mater. Struct.*, 2009, **18**(7), 074003.
- 9 K. Yu, *et al.*, Carbon nanotube chains in a shape memory polymer/carbon black composite: to significantly reduce the electrical resistivity, *Appl. Phys. Lett.*, 2011, **98**(7), 074102.
- 10 K. Yu, Y. J. Liu and J. S. Leng, Conductive Shape Memory Polymer Composite Incorporated with Hybrid Fillers: Electrical, Mechanical, and Shape Memory Properties, *J. Intell. Mater. Syst. Struct.*, 2011, **22**(4), 369–379.
- 11 A. Lendlein, *et al.*, Light-induced shape-memory polymers, *Nature*, 2005, **434**(7035), 879–882.
- 12 P. R. Buckley, *et al.*, Inductively heated shape memory polymer for the magnetic actuation of medical devices, *IEEE Trans. Biomed. Eng.*, 2006, **53**(10), 2075–2083.
- 13 R. Mohr, *et al.*, Initiation of shape-memory effect by inductive heating of magnetic nanoparticles in thermoplastic polymers, *Proc. Natl. Acad. Sci. U. S. A.*, 2006, **103**(10), 3540–3545.
- 14 A. M. Schmidt, Electromagnetic activation of shape memory polymer networks containing magnetic nanoparticles, *Macromol. Rapid Commun.*, 2006, **27**(14), 1168–1172.
- 15 K. Yu, *et al.*, Design considerations for shape memory polymer composites with magnetic particles, *J. Compos. Mater.*, 2013, **47**(1), 51–63.
- 16 W. M. Huang, *et al.*, Water-driven programmable polyurethane shape memory polymer: demonstration and mechanism, *Appl. Phys. Lett.*, 2005, **86**(11), 114105.
- 17 H. B. Lv, *et al.*, Shape-memory polymer in response to solution, *Adv. Eng. Mater.*, 2008, **10**(6), 592–595.
- 18 X. F. Luo, *et al.*, A Thermoplastic/Thermoset Blend Exhibiting Thermal Mending and Reversible Adhesion, *ACS Appl. Mater. Interfaces*, 2009, **1**(3), 612–620.
- 19 J. S. Leng, *et al.*, Comment on “Water-driven programmable polyurethane shape memory polymer: demonstration and mechanism”, *Appl. Phys. Lett.*, 2005, **86**, 114105; J. S. Leng, *et al.*, *Appl. Phys. Lett.*, 2008, **92**(20), 056101.
- 20 H. Y. Du, *et al.*, Microwave-Induced Shape-Memory Effect of Chemically Crosslinked Moist Poly(Vinyl alcohol) Networks, *Macromol. Chem. Phys.*, 2011, **212**(14), 1460–1468.
- 21 Z. H. Xu and Z. Yao, Microwave activated shape memory polymer, in *18th International conference on composite materials*, July 27th–July 31st, 2009, Edinburgh, Scotland.
- 22 Z. Guo, *et al.*, Fabrication, characterization and microwave properties of polyurethane nanocomposites reinforced with iron oxide and barium titanate nanoparticles, *Acta Mater.*, 2009, **57**(1), 267–277.
- 23 T. Hanemann and D. V. Szabo, Polymer–Nanoparticle Composites: From Synthesis to Modern Applications, *Materials*, 2010, **3**(6), 3468–3517.
- 24 C. Morales, *et al.*, Tunable Magneto-Dielectric Polymer Nanocomposites for Microwave Applications, *IEEE Trans. Microwave Theory Tech.*, 2011, **59**(2), 302–310.
- 25 H. B. Lu, *et al.*, Nanoscale Design of Nano-Sized Particles in Shape-Memory Polymer Nanocomposites Driven by Electricity, *Materials*, 2013, **6**, 3742–3754.
- 26 J. J. Li, *et al.*, Electrical Energy Storage in Ferroelectric Polymer Nanocomposites Containing Surface-Functionalized BaTiO₃ Nanoparticles, *Chem. Mater.*, 2008, **20**(20), 6304–6306.
- 27 A. Ohlan, *et al.*, Microwave absorption properties of conducting polymer composite with barium ferrite nanoparticles in 12.4–18 GHz, *Appl. Phys. Lett.*, 2008, **93**(5), 053114.
- 28 R. Saito, G. Dresselhaus and M. S. Dresselhaus, *Physical properties of carbon nanotubes*, Imperial college press, London, 1998, vol. 4.
- 29 E. Vazquez and M. Prato, Carbon Nanotubes and Microwaves: Interactions, Responses, and Applications, *ACS Nano*, 2009, **3**(12), 3819–3824.
- 30 A. Wadhawan, D. Garrett and J. M. Perez, Nanoparticle-assisted microwave absorption by single-wall carbon nanotubes, *Appl. Phys. Lett.*, 2003, **83**(13), 2683–2685.
- 31 D. Walton, H. Boehnel and D. J. Dunlop, Response of magnetic nanoparticles to microwaves, *Appl. Phys. Lett.*, 2004, **85**(22), 5367–5369.
- 32 K. R. Paton and A. H. Windle, Efficient microwave energy absorption by carbon nanotubes, *Carbon*, 2008, **46**(14), 1935–1941.
- 33 J. W. Walkiewicz, G. Kazonich and S. L. McGill, Microwave Heating Characteristics of Selected Minerals and Compounds, *Miner. Metall. Process.*, 1988, **5**, 39–42.
- 34 T. J. Imholt, *et al.*, Nanotubes in microwave fields: Light emission, intense heat, outgassing, and reconstruction, *Chem. Mater.*, 2003, **15**(21), 3969–3970.
- 35 S. Frank, *et al.*, Carbon nanotube quantum resistors, *Science*, 1998, **280**(5370), 1744–1746.

- 36 Z. Ye, *et al.*, Microwave absorption by an array of carbon nanotubes: A phenomenological model, *Phys. Rev. B: Condens. Matter Mater. Phys.*, 2006, **74**(7), 075425.
- 37 A. L. Higginbotham, *et al.*, Carbon nanotube composite curing through absorption of microwave radiation, *Compos. Sci. Technol.*, 2008, **68**(15–16), 3087–3092.
- 38 Y. Z. Fan, *et al.*, Evaluation of the microwave absorption property of flake graphite, *Mater. Chem. Phys.*, 2009, **115**(2–3), 696–698.
- 39 B. Xu, *et al.*, Thermo-mechanical properties of polystyrene-based shape memory nanocomposites, *J. Mater. Chem.*, 2010, **20**(17), 3442–3448.
- 40 Z. Spitalsky, *et al.*, Carbon nanotube–polymer composites: chemistry, processing, mechanical and electrical properties, *Prog. Polym. Sci.*, 2010, **35**(3), 357–401.
- 41 J. N. Coleman, *et al.*, Small but strong: a review of the mechanical properties of carbon nanotube–polymer composites, *Carbon*, 2006, **44**(9), 1624–1652.
- 42 W. H. Guo, *et al.*, Aligned carbon nanotube/polymer composite fibers with improved mechanical strength and electrical conductivity, *J. Mater. Chem.*, 2012, **22**(3), 903–908.
- 43 M. Cadek, *et al.*, Morphological and mechanical properties of carbon-nanotube-reinforced semicrystalline and amorphous polymer composites, *Appl. Phys. Lett.*, 2002, **81**(27), 5123–5125.
- 44 S. J. V. Frankland, *et al.*, Molecular simulation of the influence of chemical cross-links on the shear strength of carbon nanotube–polymer interfaces, *J. Phys. Chem. B*, 2002, **106**(12), 3046–3048.
- 45 A. Garg and S. B. Sinnott, Effect of chemical functionalization on the mechanical properties of carbon nanotubes, *Chem. Phys. Lett.*, 1998, **295**(4), 273–278.
- 46 J. A. Kim, *et al.*, Effects of surface modification on rheological and mechanical properties of CNT/epoxy composites, *Carbon*, 2006, **44**(10), 1898–1905.
- 47 F. H. Gojny, *et al.*, Influence of different carbon nanotubes on the mechanical properties of epoxy matrix composites – a comparative study, *Compos. Sci. Technol.*, 2005, **65**(15–16), 2300–2313.
- 48 L. Sun, *et al.*, Optimization of the Shape Memory Effect in Shape Memory Polymers, *J. Polym. Sci., Part A: Polym. Chem.*, 2011, **49**(16), 3574–3581.
- 49 W. I. Lee and G. S. Springer, Microwave Curing of Composites, *J. Compos. Mater.*, 1984, **18**(4), 387–409.
- 50 L. Outifa, *et al.*, Buildup and Optimization of a Homogeneous Microwave Curing Process for Epoxy Glass Composites, *Ind. Eng. Chem. Res.*, 1995, **34**(2), 688–698.
- 51 C. Jordan, *et al.*, Comparison of Microwave and Thermal Cure of an Epoxy-Amine Matrix, *Polym. Eng. Sci.*, 1995, **35**(3), 233–239.
- 52 V. Tartrattanakul and D. Jaroendee, Comparison between microwave and thermal curing of glass fiber-epoxy composites: effect of microwave-heating cycle on mechanical properties, *J. Appl. Polym. Sci.*, 2006, **102**(2), 1059–1070.